Systematic Study of the Role of Ligand Structure in the Formation of Homobinuclear Rhodium Macrocycles Formed via the Weak-Link Approach

Bradley J. Holliday, Pirmin A. Ulmann, Chad A. Mirkin,* and Charlotte L. Stern

Department of Chemistry and Center for Nanofabrication and Molecular Self-Assembly, 2145 Sheridan Road, Northwestern University, Evanston, Illinois 60208-3113

Lev N. Zakharov and Arnold L. Rheingold

Department of Chemistry and Biochemistry, University of California, San Diego, 9500 Gilman Drive, MC 0358, La Jolla, California 92093-0358

Received September 24, 2003

A series of new bis-1,4-phosphinoethoxyaryl hemilabile ligands of the form (1,4-(Ph_2PCH_2-$CH_2O)_2$-arene), where the nature and substituent pattern of the central arene ring have been systematically varied, is reported. These ligands were prepared in two steps by one of two synthetic routes. The reaction of each of these ligands with a highly reactive Rh(I) starting material and the resulting metastable coordination isomers have been investigated. These intermediate structures have been isolated and characterized in solution, and three complexes have been characterized in the solid state by single-crystal X-ray diffraction. The reaction investigated herein is the first step in the weak-link approach to supramolecular coordination complexes. We have utilized the resulting product distribution to glean information about the relative importance of a number of stabilizing effects associated with the metastable intermediates, including the strength of the dative heteroatom−metal bonds, metal−arene interactions, and stacking interactions between arene rings.

Introduction

The principles of coordination chemistry have been widely used to form supramolecular complexes in high yield and with a great deal of control over the architectural parameters of such structures. Most of these methods can be easily categorized into one of three general synthetic approaches: the directional-bonding,[1] symmetry-interaction,[2] and weak-link strategies.[3] The weak-link strategy utilizes the chemistry of hemilabile ligands[4] with transition metal centers to form supramolecular complexes with chemically active metals in the backbone.[5−10] This approach is carried out in two steps with the synthesis, and often isolation, of a polymetallic *metastable* synthetic intermediate structure (**a** or **b**), which precedes the formation of the target macrocycle or cage structure, Scheme 1.

The multifunctional ligands designed and synthesized for use in this approach to date have three structural features in common: (1) strong links, typically alkyldiphenylphosphine moieties, (2) weak links, typically ether, thioether, or amine moieties, and (3) rigid aromatic cores. Our group has observed the formation of two distinct coordination isomers of the metastable intermediate structures, **a** and **b**, when the ligand possesses a weak link (i.e., ether) that binds to the

* To whom correspondence should be addressed. Fax: (847) 467-5123. E-mail: camirkin@chem.northwestern.edu.

(1) (a) Leininger, S.; Olenyuk, B.; Stang, P. J. *Chem. Rev.* **2000**, *100*, 853−908. (b) Leininger, S.; Fan, J.; Schmitz, M.; Stang, P. J. *Proc. Natl. Acad. Sci. U.S.A.* **2000**, *97*, 1380−1384. (c) Cotton, F. A.; Lin, C.; Murillo, C. A. *Acc. Chem. Res.* **2001**, *34*, 759−771. (d) Fujita, M. *Struct. Bonding* **2000**, *96*, 177−201. (e) Fujita, M.; Umemoto, K.; Yoshizawa, M.; Fujita, N.; Kusukawa, T.; Biradha, K. *Chem. Commun.* **2001**, 509−518.

(2) (a) Caulder, D. L.; Raymond, K. N. *J. Chem. Soc., Dalton Trans.* **1999**, 1185−1200. (b) Caulder, D. L.; Raymond, K. N. *Acc. Chem. Res.* **1999**, *32*, 975−982. (c) Lehn, J.-M. *Supramolecular Chemistry*; VCH: New York, 1995. (d) Albrecht, M. *J. Inclusion Phenom. Macrocyclic Chem.* **2000**, *36*, 127−151. (e) Baxter, P. N. W.; Lehn, J.-M.; Baum, G.; Fenske, D. *Chem. Eur. J.* **2000**, *6*, 4510−4517.

(3) Holliday, B. J.; Mirkin, C. A. *Angew. Chem., Int. Ed.* **2001**, *40*, 2022−2043.

(4) (a) Slone, C. S.; Weinberger, D. A.; Mirkin, C. A. In *Progress in Inorganic Chemistry*; Karlin, K. D., Ed.; John Wiley & Sons: New York, 1999; Vol. 48, pp 233−250. (b) Bader, A.; Lindner, E. *Coord. Chem. Rev.* **1991**, *108*, 27−110.

(5) (a) Masar, M. S.; Ovchinnikov, M. V.; Mirkin, C. A.; Zakharov, L. N.; Rheingold, A. L. *Inorg. Chem.* **2003**, *42*, 6851−6858. (b) Gianneschi, N. C.; Bertin, P. A.; Nguyen, S. T.; Mirkin, C. A.; Zakharov, L. N.; Rheingold, A. L. *J. Am. Chem. Soc.* **2003**, *125*, 10508−10509. (c) Eisenberg, A. H.; Ovchinnikov, M. V.; Mirkin, C. A. *J. Am. Chem. Soc.* **2003**, *125*, 2836−2837. (d) Liu, X.; Stern, C. L.; Mirkin, C. A. *Organometallics* **2002**, 1017−1019. (e) Ovchinnikov, M. V.; Holliday, B. J.; Mirkin, C. A.; Zakharov, L. N.; Rheingold, A. L. *Proc. Natl. Acad. Sci. U.S.A.* **2002**, *99*, 4927−4931. (f) Liu, X.; Eisenberg, A. H.; Stern, C. L.; Mirkin, C. A. *Inorg. Chem.* **2001**, *40*, 2940−2941. (g) Eisenberg, A. H.; Dixon, F. M.; Mirkin, C. A.; Stern, C. L.; Incarvito, C. D.; Rheingold, A. L. *Organometallics* **2001**, *20*, 2051−2058. (h) Farrell, J. R.; Mirkin, C. A.; Liable-Sands, L. M.; Rheingold, A. L. *J. Am. Chem. Soc.* **1998**, *120*, 11834−11835.

(6) Holliday, B. J.; Arnold, F. P., Jr.; Mirkin, C. A. *J. Phys. Chem. A* **2003**, *107*, 2737−2742.

(7) Dixon, F. M.; Eisenberg, A. H.; Farrell, J. R.; Mirkin, C. A.; Liable-Sands, L. M.; Rheingold, A. L. *Inorg. Chem.* **2000**, *39*, 3432−3433.

(8) Farrell, J. R.; Mirkin, C. A.; Guzei, I. A.; Liable-Sands, L. M.; Rheingold, A. L. *Angew. Chem., Int. Ed.* **1998**, *37*, 465−467.

(9) Holliday, B. J.; Farrell, J. R.; Mirkin, C. A.; Lam, K.-C.; Rheingold, A. L. *J. Am. Chem. Soc.* **1999**, *121*, 6316−6317.

(10) Farrell, J. R.; Eisenberg, A. H.; Mirkin, C. A.; Guzei, I. A.; Liable-Sands, L. M.; Incarvito, C. D.; Rheingold, A. L.; Stern, C. L. *Organometallics* **1999**, *18*, 4856−4868.

10.1021/om030611a CCC: $27.50
Publication on Web 03/06/2004

Scheme 1

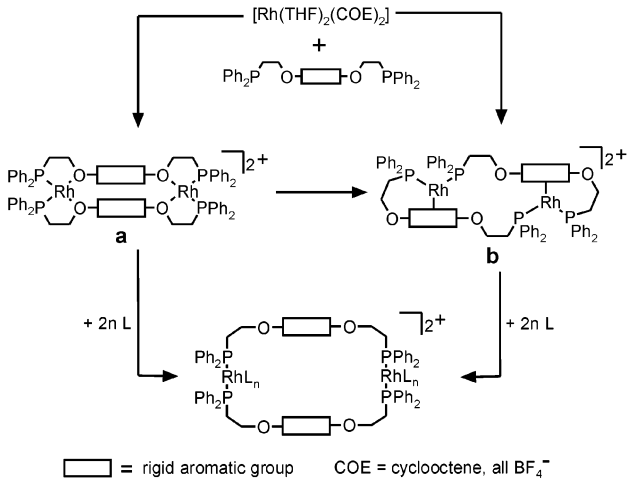

transition metal center with an affinity comparable to that of the aromatic core (i.e., benzene), Scheme 1.[10] The product distribution of these two isomers is affected by simple variations of the ligand design. For example, substitution of the ether for a stronger binding thioether results exclusively in the formation of the isomer with the thioethers bound to the metal centers (analogous to **a** in Scheme 1), a consequence of the stronger affinity of sulfur ligands for Rh(I), as compared with oxygen-containing ones.[7] However, if the heteroatoms and methylene linker length are held constant and the variation is only the nature of the aromatic group, the results are much less predictable. A number of subtle factors are varied through substitutional changes at the aromatic ring including the basicity of the weak binding groups (e.g., the oxygen atoms or arenes), the strength of the $\pi-\pi$ interactions in structure **a**, the strength of the arene−metal bond in structure **b**, and the steric contributions of the various ligand components that make up the resulting intermediate complex. This study is aimed at elucidating the relative importance of these effects in determining the metal coordination environment of the intermediate formed in the first step of the weak-link approach (i.e., either **a** or **b**, Scheme 1). To this end, a series of new phosphinoalkyl ether ligands that differ in substitution of the aromatic core has been synthesized, Figure 1. The reactivity patterns of these ligands with a Rh(I) starting material are discussed herein.

Results

Synthesis of Ligands 8−11, 13, and 16. The ligands used in this study were prepared in two synthetic steps. The oxygen atoms of the central ring are initially alkylated to generate aromatic diethers with alkyl halide ends. These intermediates are then converted to the target ligands by substitution of the halides with potassium diphenylphosphide, Scheme 2. The initial alkylations to form the ligand precursors were performed by one of two routes depending on whether the starting materials were commercially available in the quinone or hydroquinone forms. Hydroquinones were functionalized via a substitution reaction performed with potassium carbonate as the base in the presence of a large excess of 1,2-dichloroethane, route 1 in

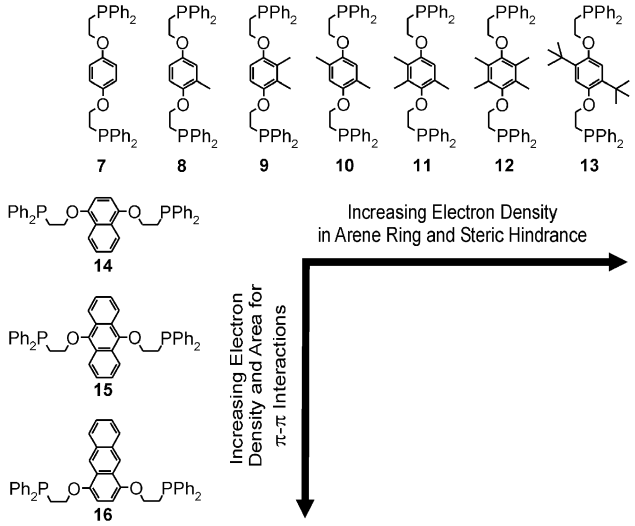

Figure 1. Hemilabile ligands used in the weak-link approach.

Scheme 2. The preparation from the quinone starting materials was accomplished via a one-pot reductive alkylation procedure.[11] Sodium hydrosulfite was used as the reducing agent, and 2-chloroethyl *p*-toluenesulfonate was the alkylating reagent, route 2 in Scheme 2. The target ligands were then synthesized in moderate to high yield (60−90%), depending on ligand type, by nucleophilic substitution of the chloro precursors with potassium diphenylphosphide. All spectroscopic, high-resolution mass spectrometry, and combustion analysis data for **8**−**11**, **13**, and **16** and the corresponding ethoxychloro precursors are consistent with the proposed structures (vide infra).

Synthesis of Rh(I) Complexes. The binuclear Rh(I) complexes were prepared in near quantitative yield by the reaction of the appropriate ligand with a highly reactive rhodium solvent adduct, which is generated by the reaction of $[RhCl(COE)_2]_2$ and $AgBF_4$ in dichloromethane followed by the addition of THF, Scheme 3. The reactions are carried out at reduced temperature (−78 °C) and under dilute conditions (0.4 mM) to avoid formation of polymeric or oligomeric materials. Our group has reported analogous synthetic procedures with other ligand systems.[10] The binuclear condensed intermediate complexes are isolated by the removal of the solvent and precipitation of the metal-containing species from a dichloromethane solution with pentane or diethyl ether, which removes the displaced COE ligand, the only biproduct of this reaction. Care was taken to keep reaction conditions consistent throughout the series of reactions reported in this study. The product distribution can then be determined by $^{31}P\{^1H\}$ NMR and ^1H NMR spectroscopies and ESI (electrospray ionization) mass spectrometry. The $^{31}P\{^1H\}$ NMR spectroscopy of this class of metal complexes is extremely diagnostic of the assigned structures. Chemical shift and Rh−P coupling constant data are available for a large number of analogous complexes, allowing for unambiguous assignments.[5,7−10]

The two possible coordination isomers of the product can be easily differentiated by $^{31}P\{^1H\}$ NMR spectros-

(11) Kraus, G. A.; On Man, T. *Synth. Commun.* **1986**, *16*, 1037−1042.

Scheme 2

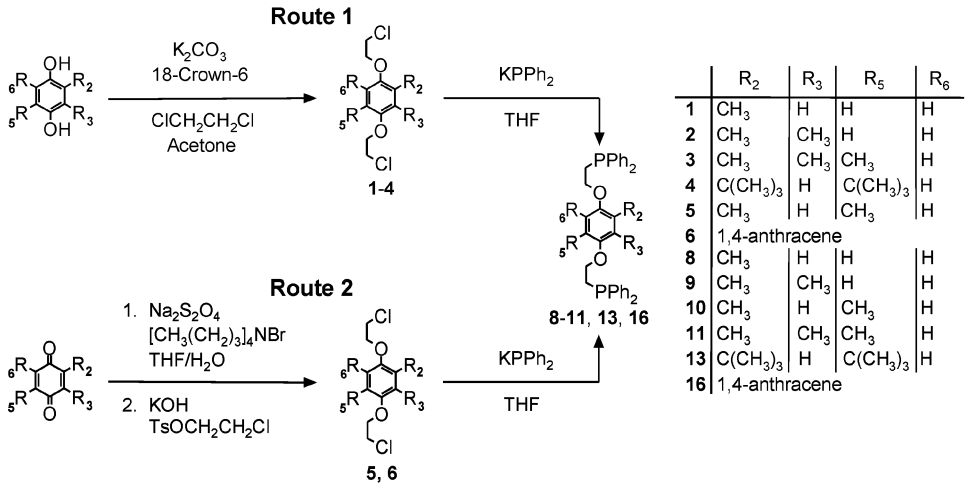

	R_2	R_3	R_5	R_6
1	CH_3	H	H	H
2	CH_3	CH_3	H	H
3	CH_3	CH_3	CH_3	H
4	$C(CH_3)_3$	H	$C(CH_3)_3$	H
5	CH_3	H	CH_3	H
6	1,4-anthracene			
8	CH_3	H	H	H
9	CH_3	CH_3	H	H
10	CH_3	H	CH_3	H
11	CH_3	CH_3	CH_3	H
13	$C(CH_3)_3$	H	$C(CH_3)_3$	H
16	1,4-anthracene			

Scheme 3

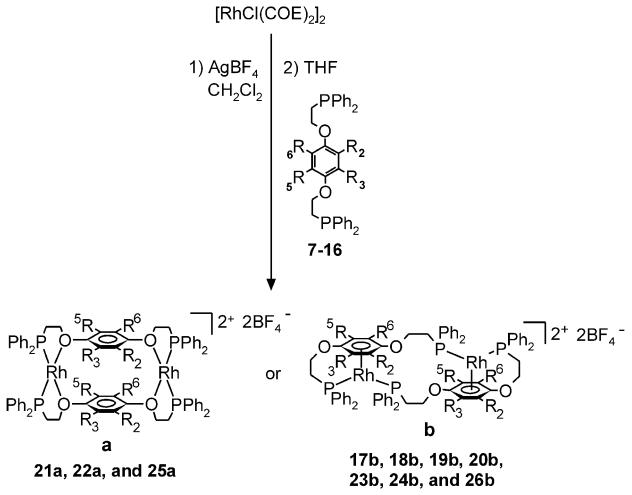

	R_2	R_3	R_5	R_6
17b	H	H	H	H
18b	CH_3	H	H	H
19b	CH_3	CH_3	H	H
20b	CH_3	H	CH_3	H
21a	CH_3	CH_3	CH_3	H
22a	CH_3	CH_3	CH_3	CH_3
23b	$C(CH_3)_3$	H	$C(CH_3)_3$	H
24b	1,4-naphthalene			
25a	9,10-anthracene			
26b	1,4-anthracene			

copy. For example, the $^{31}P\{^1H\}$ NMR spectrum of the bow-tie intermediate structure, **a**, exhibits a single doublet (when the ligand possesses equivalent phosphine groups) at δ ~60 with a Rh−P coupling constant in the 200−215 Hz range, indicative of *cis*-ether, *cis*-phosphine coordination environments around the rhodium(I) metal centers. In contrast, the slipped intermediate structure, **b**, displays two resonances in its $^{31}P\{^1H\}$ NMR spectrum (δ ~18−35) due to inequivalent phosphines. In this case, the two $^{31}P\{^1H\}$ NMR resonances display a distinct coupling pattern consisting of a doublet of doublets, which derives from P−P ($J_{P-P} \approx$ 40 Hz) and Rh−P ($J_{Rh-P} \approx$ 200 Hz) coupling. The coordination isomers observed for each respective ligand are summarized in Scheme 3.

Notably, both possible isomers (slipped and bow-tie) of the metal complexes synthesized from ligands **8**, **10**, **11**, and **13** have the potential to form as racemic mixtures of chiral metal complexes depending on the relative orientation of the substituents on the arene ring in the Rh(I) product. More specifically, if the substituents and gaps (hydrogen positions) around the arene rings interdigitate, as opposed to stack directly on top of one another, the resulting complex will be chiral. No time or consideration was given to the resolution of these mixtures of enantiomers, as the reaction of any of these intermediate products with ancillary ligands to form the open macrocyclic structures results in the free rotation of the arene groups and loss of chirality, Scheme 1.

X-ray Crystallography of 18b. Red crystals suitable for X-ray study were grown by slow diffusion of pentane into a saturated solution of **18b** in dichloromethane at room temperature. One dichloromethane and one pentane molecule cocrystallized with **18b**. Selected bond lengths and angles in **18b** are given in Table 1, and the crystallographic data are listed in Table 2. The relative orientation of the substituents on the arene rings in complex **18b** was confirmed in the solid state by an X-ray diffraction study, Figure 2. In the solid state, the two methyl substituents on the central arene ring adopt a *syn* conformation relative to each other. However, the methyl group is disordered equally between the 2- and 3-position on the arene ring, indicating that **18b** exists as a mixture of isomers in solution which cocrystallize. The Rh(I) metal centers display expected bis-phosphine, η^6-arene, two-legged piano stool coordination geometries in the solid state and exhibit Rh(I)−C bond lengths (2.258(10)−2.433(8) Å) in the range previously reported for compounds with similar coordination environments (Table 1).[10] The two rhodium metal centers are 7.45 Å apart, and the Rh−P bond lengths ($Rh-P(chelating)_{av}$ = 2.231(2) Å and $Rh-P(bridging)_{av}$ = 2.249(2) Å) are slightly shorter than those in complex **17b**, the unsubstituted arene analogue that has been previously reported ($Rh-P(chelating)_{av}$ = 2.274 Å and $Rh-P(bridging)_{av}$ = 2.296 Å).[10] The shortening of these bonds leads to the widening of the P−Rh−P bond angle (95.13(8)°) relative to **17b** (95.06°).

X-ray Crystallography of 19b. Crystals of **19b** for X-ray study were grown by slow diffusion of diethyl ether into a concentrated solution of **19b** in dichloromethane at room temperature. Several solvent molecules (five ether and two dichloromethane) cocrystal-

Table 1. Selected Bond Distances (Å) and Bond Angles (deg) for 18b, 19b, and 23b

18b		19b		23b	
Rh1−P1	2.236(2)	Rh1−P1	2.2243(16)	Rh1−P1	2.2299(10)
Rh1−P2	2.240(2)	Rh1−P2	2.2471(14)	Rh1−P2	2.2668(9)
Rh2−P3	2.259(3)	Rh2−P3	2.2333(15)	Rh1−C1	2.445(3)
Rh2−P4	2.2269(19)	Rh2−P4	2.2436(13)	Rh1−C2	2.437(3)
Rh1−C1	2.363(10)	Rh1−C1	2.258(6)	Rh1−C3	2.338(3)
Rh1−C2	2.432(8)	Rh1−C2	2.239(5)	Rh1−C4	2.397(4)
Rh1−C3	2.405(9)	Rh1−C3	2.368(6)	Rh1−C5	2.245(3)
Rh1−C4	2.293(11)	Rh1−C4	2.389(6)	Rh1−C6	2.239(3)
Rh1−C5	2.261(10)	Rh1−C5	2.397(6)	P1−Rh1−P2	97.38(3)
Rh1−C6	2.356(10)	Rh1−C6	2.387(6)		
Rh2−C39	2.359(10)	Rh2−C13	2.255(5)		
Rh2−C40	2.262(11)	Rh2−C14	2.308(6)		
Rh2−C41	2.258(10)	Rh2−C15	2.393(6)		
Rh2−C42	2.359(7)	Rh2−C16	2.416(6)		
Rh2−C37	2.419(7)	Rh2−C17	2.398(6)		
Rh2−C38	2.402(9)	Rh2−C18	2.377(6)		
P1−Rh1−P2	94.85(8)	P1−Rh1−P2	94.92(6)		
P3−Rh2−P4	95.41(8)	P3−Rh2−P4	94.86(5)		

Table 2. Crystallographic Data for 18b, 19b, and 23b

	18b	19b	23b
formula	$C_{70}H_{68}B_2F_8O_4P_4Rh_2 \cdot 0.5(CH_2Cl_2) \cdot 0.5(C_5H_{12})$	$C_{72}H_{72}B_2F_8O_4P_4Rh_2 \cdot 2(CH_2Cl_2) \cdot 5(C_4H_{10}O)$	$C_{84}H_{96}B_2F_8O_4P_4Rh_2 \cdot 6(CH_2Cl_2) \cdot C_4H_{10}O$
fw	1548.04	2045.07	2256.72
color, habit	red, block	red, block	red, block
cryst dimens (mm)	0.28 × 0.15 × 0.14	0.25 × 0.20 × 0.15	0.25 × 0.20 × 0.10
space group	*Cc*	*Cc*	*I*2/*a*
cryst syst	monoclinic	monoclinic	monoclinic
a, Å	23.571(4)	23.0417(12)	23.097(2)
b, Å	26.920(5)	29.121(2)	14.5217(12)
c, Å	16.234(3)	16.1785(8)	28.715(4)
α, deg	90	90	90
β, deg	129.141(2)	128.332(1)	94.639(1)
γ, deg	90	90	90
V, Å^3	7989.3(23)	8515.4(9)	9599.7(17)
Z, *Z*′	4, 1	4, 1	4, 0.5
D_{calcd}, g cm^{-3}	1.287	1.595	1.561
radiation (*λ*, D)	Mo Kα (0.71069)	Mo Kα (0.71073)	Mo Kα (0.71073)
F(000)	3148	4248	4632
2*θ* range, deg	2.70−56.5	2.66−56.58	3.32−56.64
μ, cm^{-1}	0.588 (Mo Kα)	0.67 (Mo Kα)	0.81 (Mo Kα)
range of transmn factors	0.691315−1.00	0.83−1.00	0.693−1.00
T, K	153(2)	128(2)	150(2)
scan method	*ω*	*ω*	*ω*
abs corr		empirical from SADABS	
no. of measd reflns	36 328	27 122	28 927
no. of indep reflns	18 093 [R_{int} = 0.0614]	12 563 [R_{int} = 0.0316]	11 107 [R_{int} = 0.0508]
refinement method		full-matrix least-squares on F^2	
GOF on F^2	1.01	1.035	0.963
final *R* indices[a] ($I > 2\sigma(I)$)	R1 = 0.0764, wR2 = 0.1978	R1 = 0.0497, wR2 = 0.1349	R1 = 0.0563, wR2 = 0.1438
R indices (all data)	R1 = 0.1201, wR2 = 0.2357	R1 = 0.0531, wR2 = 0.1378	R1 = 0.0771, wR2 = 0.1510

[a] $R1 = \sum||F_o| - |F_c||/\sum|F_o|$, $wR2 = [\sum(w(F_o^2 - F_c^2)^2)/\sum w(F_o^2)^2]^{1/2}$, $w = 1/\sigma^2(F^2)$.

lized with **19b**. The X-ray diffraction study confirms the slipped geometry observed in solution and shows that the methyl groups on the two arene rings are oriented in a *syn* fashion, Figure 3, Table 1 and Table 2. The coordination geometry around the Rh(I) metal center is similar to that observed for **18b** (vide supra) and is consistent with the geometry of the previous literature examples of this class of compound.[10] The rhodium−carbon bond distances (2.239(5)−2.416(6) Å) are in line with previously reported values for η^6-bound arene rings in a bis-phosphine two-legged piano-stool geometry.[10,12] Surprisingly, the average Rh−C bond lengths in structures **18b** and **19b** are identical within experimental error (2.34(9) and 2.34(7) Å, respectively). This suggests that the addition of one methyl group to the arene ring on going from ligand **8** to **9** has a very minor affect, if any, on the strength of the Rh−arene bond. The Rh(I) metal centers are positioned 7.49 Å apart in structure **19b**. Finally, inspection of the Rh−P bond lengths (Rh−P(chelating)$_{av}$ = 2.229(6) Å and Rh−P(bridging)$_{av}$ = 2.245(2) Å) and P−Rh−P bond angle (94.89(4)°) in

(12) (a) Dixon, F. M.; Masar, M. S., III; Doan, P. E.; Farrell, J. R.; Arnold, F. P., Jr.; Mirkin, C. A.; Incarvito, C. D.; Zakharov, L. N.; Rheingold, A. L. *Inorg. Chem*. **2003**, *42*, 3245−3255. (b) Dixon, F. M.; Farrell, J. R.; Doan, P. E.; Williamson, A.; Weinberger, D. A.; Mirkin, C. A.; Stern, C.; Incarvito, C. D.; Liable-Sands, L. M.; Zakharov, L. N.; Rheingold, A. L. *Organometallics* **2002**, *21*, 3091−3093. (c) Singewald, E. T.; Shi, X.; Mirkin, C. A.; Schofer, S. J.; Stern, C. L. *Organometallics* **1996**, *15*, 3062−3069. (d) Slone, C. S.; Mirkin, C. A.; Yap, G. P. A.; Guzei, I. A.; Rheingold, A. L. *J. Am. Chem. Soc.* **1997**, *119*, 10743−10753. (e) Alvarez, M.; Lugan, N.; Donnadieu, B.; Mathieu, R. *Organometallics* **1995**, *14*, 365−370. (f) Westcott, S. A.; Taylor, N. J.; Marder, T. B.; Baker, R. T.; Jones, N. J.; Calabrese, J. C. *Chem. Commun*. **1991**, 304−305. (g) Townsend, J. M.; Blount, J. F. *Inorg. Chem*. **1981**, *20*, 269−271. (h) Albano, P.; Aresta, M.; Manassero, M. *Inorg. Chem*. **1980**, *19*, 1069−1072. (i) Singewald, E. T.; Slone, C. S.; Stern, C. L.; Mirkin, C. A.; Yap, G. P. A.; Liable-Sands, L. M.; Rheingold, A. L. *J. Am. Chem. Soc.* **1997**, *119*, 3048−3056.

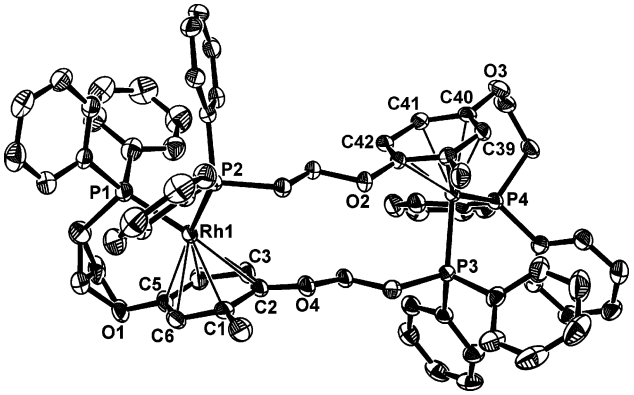

Figure 2. ORTEP diagram of complex **18b**. Thermal ellipsoids are drawn at 50% probability. Hydrogen atoms, solvent molecules, and anions are omitted for clarity. See Table 1 for selected bond distances and angles.

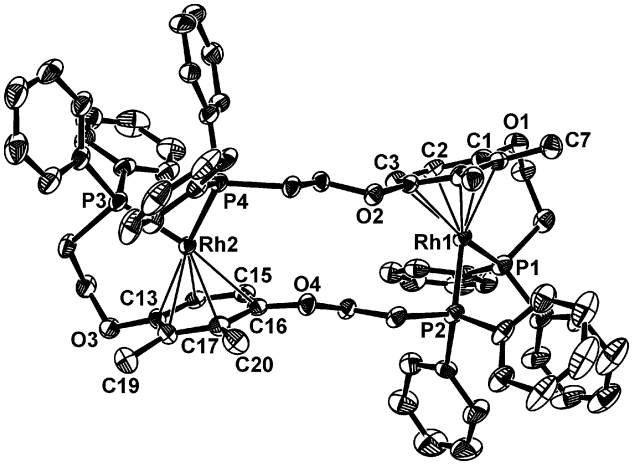

Figure 3. ORTEP diagram of complex **19b**. Thermal ellipsoids are drawn at 50% probability. Hydrogen atoms, solvent molecules, and anions are omitted for clarity. See Table 1 for selected bond distances and angles.

structure **19b**, and comparison with those for **18b**, reveals that the Rh−P bonds are significantly shorter (0.05 Å) in the dimethyl structure, while the P−Rh−P angle in **19b** is only slightly smaller.

X-ray Crystallography of 23b. Crystals for X-ray diffraction study were grown by slow diffusion of diethyl ether into a concentrated dichloromethane solution of **23b** at room temperature, Figure 4. Several solvent molecules (six CH_2Cl_2 and one ether) cocrystallized with **23b** and were observed in the solid-state structure. The crystal structure determination confirms that **23b** is the slipped isomer and displays the expected arene-bound Rh(I) metal centers, Figure 4. The Rh−C bond lengths (2.239(3)−2.445(3) Å) are consistent with the previously observed Rh−C distances in other arene-bound Rh(I) complexes[10,12] and compare well with the values found in structures **18b** and **19b**. The Rh−P bonds lengths (Rh−P(chelating) = 2.2299(10) Å and Rh−P(bridging) = 2.268(9) Å) are also consistent with the Rh−P bond lengths previously observed for examples of complexes with similar coordination environments and agree well with the analogous bond lengths in structures **18b** and **19b**. The solid-state structure of **23b** reveals that the bulky *tert*-butyl groups are oriented in an alternating fashion, a likely consequence of the bow-tie structure, **a**, that presumably forms before the slipped intermediate, **b** (vide infra), Figure 5. To avoid eclipsing interactions in the bow-tie structure, **a**, the ligands must adopt this conformation in which the substituents are interdigitated instead of stacked on top of one another, Figure 5. This is in contrast with structures **18b** and **19b**, in which the substituents are in a *syn* conformation and would therefore be overlapping in a ring-stacked geometry due to favorable van der Waals interactions between the methyl substituents. The arrangement of the *tert*-butyl groups in this fashion in structure **23b** makes the complex chiral, and both enantiomers are in the crystal structure.

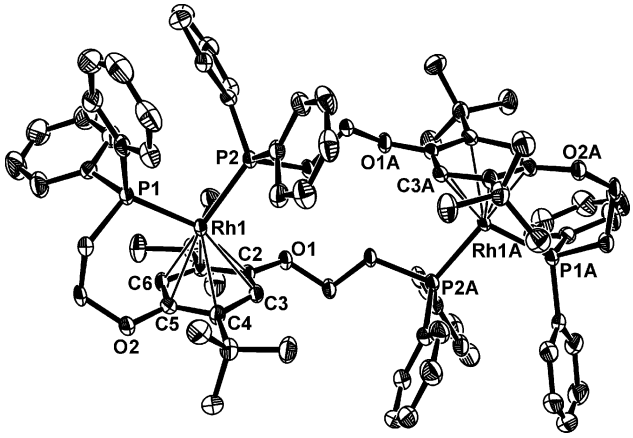

Figure 4. ORTEP diagram of complex **23b**. Thermal ellipsoids are drawn at 50% probability. Hydrogen atoms, solvent molecules, and anions are omitted for clarity. See Table 1 for selected bond distances and angles.

Discussion

The ligands reported in this article were designed to evaluate the factors that control the formation of one of two possible intermediates, **a** and **b**, formed via the weak-link approach, Scheme 1. Regardless of what is ultimately observed and characterized as the metastable intermediate, based upon these studies and previous ones,[5−10] we believe that the system enters the binuclear manifold by first forming the bow-tie intermediate **a**. The type of ligand employed in the approach dictates which intermediate resting state will be observed (i.e., **a** or **b**, Figure 6). When combined with the data from previous studies,[9,10,13] the data for the ligands studied herein allow one to outline trends in reactivity that stem from the subtle changes in steric and electronic factors associated with the ligands.

A series of new phosphinoalkyl ether-based ligands, which consists of a systematic variation of the substituents on the central arene ring, has been synthesized, Figure 1. The changes made to the ligands can affect how the arene ring interacts with a metal center in several ways. While the phosphine portions of the ligands are not affected by these changes, as evidenced by the virtually identical $^{31}P\{^1H\}$ NMR chemical shifts for all of the ligands, the oxygen basicity, metal−arene affinity, and arene−arene interactions are all modified by changes to the arene ring in the center of the ligand. Indeed, some of these effects are additive, and some are

(13) Holliday, B. J.; Jeon, Y.-M.; Mirkin, C. A.; Stern, C. L.; Incarvito, C. D.; Zakharov, L. N.; Sommer, R. D.; Rheingold, A. L. *Organometallics* **2002**, *21*, 5713−5725.

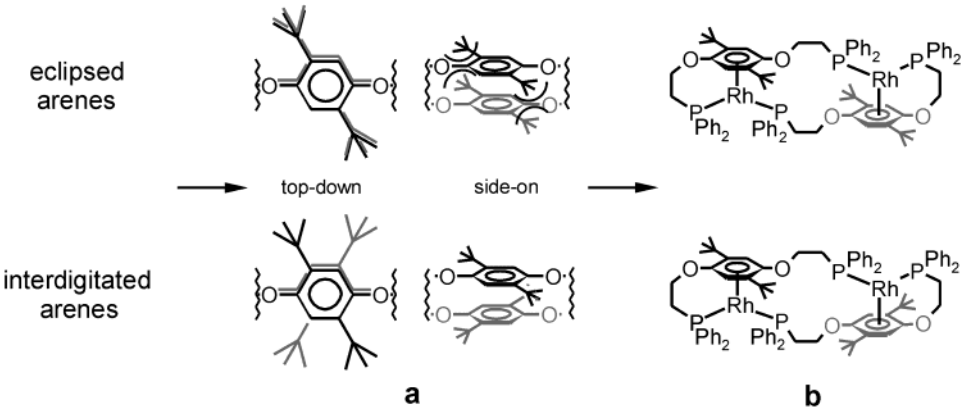

Figure 5. Two relative arene orientations in isomers **a** and **b**.

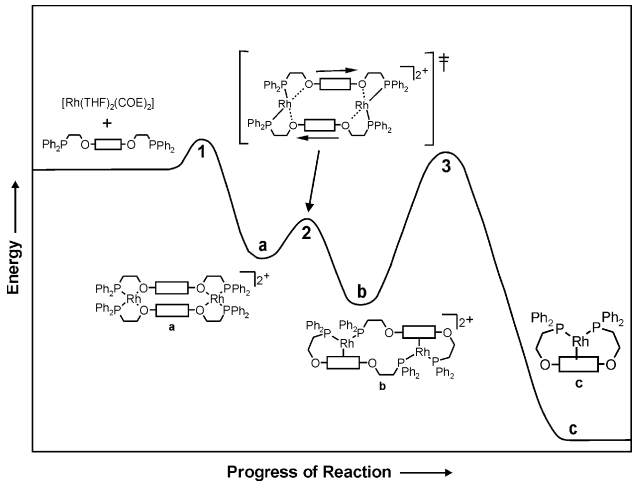

Figure 6. Relative energetics of the weak-link approach.

canceling. For example if one considers the two extremes of the series, on going from the benzene-based ligand to the durene-based ligand the basicity of the oxygens and the potential for van der Waals interactions between two stacked and interdigitated arene rings are enhanced by increasing the number of electron-donating aliphatic substituents on the arene rings; this would favor formation of the bow-tie structure, **a**. However, this change also would be expected to increase the arene−Rh(I) interaction, which would favor the slipped isomer, **b**. On the basis of the experimentally observed product distributions reported herein combined with previously reported results,[9,10,13] a better understanding of the relative reaction pathways can be developed, Figure 6. Below, we systematically examine each of the possible contributing effects to intermediate isomer formation.

Ring−Ring Interactions. On the basis of experimental and theoretical studies, the strength of the arene−arene interaction can be estimated to be 2−5 kcal/mol, depending on the type of substitution.[14] This interaction certainly plays a minor role in determining the relative stabilities of intermediates **a** and **b**, but it seems to play a more significant role in the initial organization of the starting materials, transition state 1, Figure 6. The binding and chelation events between the metals and ligands are the predominate effects in the organization of the starting materials, but the ring−ring interactions serve to stabilize the bow-tie structure once it is formed. Evidence for this can be gleaned from the X-ray crystal structures of the slipped structures reported herein and previously. Specifically, the observation that every ligand that has been used which is unsymmetric along the oxygen−oxygen axis (i.e., **8**, **9**, **11**, and **16**) forms exclusively the *syn* conformation in the condensed intermediate. This preference displays the positive stabilization present between the two rings and their respective substituents in transition state 1, Figure 6.

Metal−Oxygen Interaction. While the two intermediates in the weak-link approach are kinetic products relative to the monomeric species, Figure 6, the slipped isomer, **b**, is more thermodynamically stable than the bow-tie isomer, **a**, at least for the systems studied thus far. This is supported by the observation that, in certain ligand systems, the bow-tie isomer can be isolated and characterized but upon heating converts cleanly to the slipped structure.[10,13] We believe that all of these intermediate structures pass through the bow-tie intermediate **a**, and the strength of the metal−oxygen interaction is what determines the product that is ultimately observed (**a** or **b**). Indeed, the strength of this interaction, coupled with the cumulative van der Waals interactions between the arene rings in **a**, is what predominantly determines the height of barrier 2, Figure 6.

Metal−Arene Interaction. The metal−arene interaction present in the slipped intermediate is a relatively strong stabilizing force, especially in the chelating environment of such a geometrically constrained system. For the systems studied thus far, this interaction is the one that leads to the slipped intermediate being the most energetically favorable of the two possible structures. This also leads to a high activation barrier to monomer formation, which is in large part the premise behind the weak-link approach. Indeed, one can open the intermediate structures to form desired macrocycles without forming monomer as long one works at room temperature.

Conclusions

A new series of phosphinoalkyl ether ligands with different aromatic core groups has been synthesized and

(14) (a) Hunter, C. A.; Lawson, K. R.; Perkin, J.; Urch, C. J. *J. Chem. Soc., Perkin Trans. 2* **2001**, 651−669. (b) Gonzalez, C.; Lim, E. C. *Chem. Phys. Lett.* **2000**, *322*, 382−388. (c) Sinnokrot, M. O.; Valeev, E. F.; Sherrill, C. D. *J. Am. Chem. Soc.* **2002**, *124*, 10887−10893. (d) Tsuzuki, S.; Honda, K.; Uchimaru, T.; Mikami, M.; Tanabe, K. *J. Am. Chem. Soc.* **2002**, *124*, 104−112.

characterized, and these ligands have been used to carry out a systematic study of how ligand substitution affects the reaction pathway of the weak-link approach. The trends reported here lend qualitative insight into some of the factors controlling the weak-link approach and allow the following conclusions to be made: (1) the $\pi-\pi$ stacking and van der Waals interactions between the aromatic rings in the ligands are of minor importance in the organization of starting materials but do contribute to the adopted orientation of the arenes relative to each other in the final product; (2) the magnitude of the metal−oxygen bond strengths in structure **a** is an extremely important factor in stabilizing this structure and the predominant effect governing the coordination isomer that is observed; and (3) the metal−arene interactions in structure **b** are important stabilizing factors and can be directly affected by the substituents around the arene core.

Experimental Section

General Methods. Unless otherwise noted, all reactions and manipulations were carried out under nitrogen using standard Schlenk techniques or in an inert-atmosphere glovebox. Methylene chloride, pentane, cyclohexane, and acetonitrile were dried over calcium hydride. Tetrahydrofuran and diethyl ether were dried over sodium/benzophenone. All solvents were distilled under nitrogen and degassed via nitrogen purge prior to use. Deuterated solvents were purchased from Cambridge Isotope Laboratories and used without further purification. $RhCl_3 \cdot xH_2O$ was purchased from Colonial Metals, Inc., and $[RhCl(COE)_2]_2$ (COE = cyclooctene) was synthesized according to literature methods.[15] All other chemicals were purchased from commercial sources and used as received. Chromatography grade silica gel (0.040−0.063 mm, 230−400 mesh ASTM, EM Science) and neutral activated alumina (150 mesh, 58 Å, Aldrich) were used for chromatography. Elemental analyses were performed by QTI, Whitehouse, NJ (www.qtionline.com). The synthesis and characterization of compounds **7**, **12**, **14**, **15**, **17**, **22**, **24**, and **25** have been previously reported.[8−10]

Instrumental Details. NMR spectra were recorded on a Varian Gemini 300 MHz spectrometer. ^{1}H NMR signals are reported relative to residual proton resonances in deuterated solvents. The $^{31}P\{^1H\}$ NMR spectra were recorded at 121 MHz and referenced versus an 85% H_3PO_4 external standard. All NMR resonances are reported in ppm, and coupling constants are given in Hz. $^{13}C\{^1H\}$ NMR spectra were recorded at 75 MHz and referenced relative to solvent peaks. Electron impact (EI) mass spectra were recorded using a Fisions VG 70-250 SE mass spectrometer, and electrospray (ES) mass spectra were recorded on a Micromass Quatro II electrospray triple quadrapole mass spectrometer. Melting points were recorded on a Mel-Temp II melting temperature apparatus made by Laboratory Devices of Holliston, MA.

General Procedure for the Synthesis of Di(2-chloroethoxy)arenes from Hydroquinones (1−4). A mixture of hydroquinone (25.5 mmol), potassium carbonate (20 g, 145 mmol), and 18-crown-6 (1.0 g, 3.8 mmol) was suspended in a mixture of 1,2-dichloroethane (40 mL) and acetone (10 mL). The reaction mixture was then brought to reflux with vigorous stirring for 2 days. After cooling to RT, the mixture was filtered through a pad of Celite and silica gel before the solvent was removed in vacuo. The resulting oily solid was dried under vacuum, which resulted in solidification. The crude solid was titrated with a small amount of ethanol (25 mL), collected by filtration, and dried under vacuum to give analytically pure product.

(15) *Reagents for Transition Metal Complex and Organometallic Synthesis*; John Wiley & Sons: New York, 1990; Vol. 28.

1,4-Di(2-chloroethoxy)-2-methylbenzene (1). Yield = 72%; mp 51.6−52.0 °C. ^{1}H NMR: ($CDCl_3$) 6.79−6.68 (m, C_6H_3, 3H), 4.19 (t, OCH_2, J_{H-H} = 5.9, 2H), 4.18 (t, OCH_2, J_{H-H} = 5.7, 2H), 3.81 (t, CH_2Cl, J_{H-H} = 6.2, 2H), 3.79 (t, CH_2Cl, J_{H-H} = 6.2, 2H), 2.25 (s, CH_3, 3H). $^{13}C\{^1H\}$ NMR: ($CDCl_3$) 152.7 (s, $C_{1/4}$), 151.3 (s, $C_{1/4}$), 129.1 (s, C_2), 118.3 (s, C_3), 113.2 (s, $C_{5/6}$), 112.4 (s, $C_{5/6}$), 69.3 (s, OCH_2), 68.9 (s, OCH_2), 42.4 (s, CH_2Cl), 42.2 (s, CH_2Cl), 16.5 (s, CH_3). HRMS (EI, *m*/*z*): calcd for $C_{11}H_{14}Cl_2O_2$ 248.0371 (M^+), found 248.0371 (M^+). Anal. Calcd for $C_{11}H_{14}Cl_2O_2$: C, 53.22; H, 5.69. Found: C, 53.35; H, 5.84.

1,4-Di(2-chloroethoxy)-2,3-dimethylbenzene (2). Yield = 97%; mp 42.0−42.3 °C. ^{1}H NMR: ($CDCl_3$) 6.66 (s, C_6H_2, 2H), 4.18 (t, OCH_2, J_{H-H} = 5.9, 4H), 3.82 (t, CH_2Cl, J_{H-H} = 5.9, 4H), 2.20 (s, CH_3, 6H). $^{13}C\{^1H\}$ NMR: ($CDCl_3$) 151.2 (s, $C_{1/4}$), 128.1 (s, $C_{2/3}$), 110.3 (s, $C_{5/6}$), 69.5 (s, OCH_2), 42.5 (s, CH_2Cl), 12.4 (s, CH_3). HRMS (EI, *m*/*z*): calcd for $C_{12}H_{16}Cl_2O_2$ 262.0527 (M^+), found 262.0527 (M^+). Anal. Calcd for $C_{12}H_{16}Cl_2O_2$: C, 54.77; H, 6.13. Found: C, 54.69; H, 6.15.

1,4-Di(2-chloroethoxy)-2,3,5-trimethylbenzene (3). Yield = 68%; mp 45.1−45.6 °C. ^{1}H NMR: ($CDCl_3$) 6.53 (s, C_6H, 1H), 4.18 (t, OCH_2, J_{H-H} = 5.7, 2H), 3.96 (t, OCH_2, J_{H-H} = 5.7, 2H), 3.82 (m, CH_2Cl, 4H), 2.28 (s, CH_3, 3H), 2.22 (s, CH_3, 3H), 2.15 (s, CH_3, 3H). $^{13}C\{^1H\}$ NMR: ($CDCl_3$) 152.6 (s, $C_{1/4}$), 149.4 (s, $C_{1/4}$), 131.1 (s, C_3), 128.2 (s, C_5), 124.9 (s, C_2), 112.4 (s, C_6), 72.4 (s, OCH_2), 69.1 (s, OCH_2), 43.2 (s, CH_2Cl), 42.5 (s, CH_2-Cl), 16.7 (s, C_5-CH_3), 13.1 (s, C_2-CH_3), 12.2 (s, C_3-CH_3). HRMS (EI, *m*/*z*): calcd for $C_{13}H_{18}Cl_2O_2$ 276.0684 (M^+), found 276.0690 (M^+). Anal. Calcd for $C_{13}H_{18}Cl_2O_2$: C, 56.51; H, 6.57. Found: C, 56.61; H, 6.69.

1,4-Di(2-chloroethoxy)-2,5-di-*tert*-butylbenzene (4). Yield = 73%; mp 125.8−126.1 °C. ^{1}H NMR: ($CDCl_3$) 6.80 (s, C_6H_2, 2H), 4.26 (t, OCH_2, J_{H-H} = 5.7, 4H), 3.88 (t, CH_2Cl, J_{H-H} = 5.7, 4H), 1.40 (s, CH_3, 18H). $^{13}C\{^1H\}$ NMR: ($CDCl_3$) 150.8 (s, $C_{1/4}$), 136.6 (s, $C_{2/5}$), 112.1 (s, $C_{3/6}$), 68.7 (s, OCH_2), 42.7 (s, CH_2-Cl), 34.9 (s, $C(CH_3)_3$), 30.1 (s, CH_3). HRMS (EI, *m*/*z*): calcd for $C_{18}H_{28}Cl_2O_2$ 346.1466 (M^+), found 346.1463 (M^+). Anal. Calcd for $C_{18}H_{28}Cl_2O_2$: C, 62.25; H, 8.13. Found: C, 62.09; H, 8.05.

General Procedure for the Synthesis of Di(2-chloroethoxy)arenes from Quinones (5, 6). A mixture of quinone (20.0 mmol), sodium hydrosulfite (20.89 g, 120 mmol), and tetrabutylammonium bromide (0.75 g, 2.3 mmol) was suspended in a mixture of THF (50 mL) and water (30 mL) and stirred at RT for 15 min. Potassium hydroxide (25.8 g, 460 mmol) was dissolved in 20 mL of water and added to the reaction mixture followed by the syringe addition of the 2-chloroethyl *p*-toluenesulfonate (23.5 mL, 130 mmol). The reaction mixture was heated to reflux for 4 h before being cooled to RT, extracted with CH_2Cl_2 from water, dried over $MgSO_4$, and collected as a crude oily solid by removal of the solvent by vacuum evaporation. The crude solid was washed with ethanol and dried under vacuum, yielding analytically pure product.

1,4-Di(2-chloroethoxy)-2,5-dimethylbenzene (5). Yield = 50%; mp 94.3−94.8 °C. ^{1}H NMR: ($CDCl_3$) 6.66 (s, C_6H_2, 2H), 4.19 (t, OCH_2, J_{H-H} = 6.0, 4H), 3.81 (t, CH_2Cl, J_{H-H} = 6.0, 4H), 2.23 (s, CH_3, 6H). $^{13}C\{^1H\}$ NMR: ($CDCl_3$) 150.8 (s, $C_{1/4}$), 125.6 (s, $C_{2/5}$), 115.8 (s, $C_{3/6}$), 69.5 (s, OCH_2), 42.5 (s, CH_2Cl), 16.2 (s, CH_3). HRMS (EI, *m*/*z*): calcd for $C_{12}H_{16}Cl_2O_2$ 262.0527 (M^+), found 262.0528 (M^+). Anal. Calcd for $C_{12}H_{16}Cl_2O_2$: C, 54.77; H, 6.13. Found: C, 54.96; H, 6.11.

1,4-Di(2-chloroethoxy)anthracene (6). Yield = 40%; mp 115−116 °C. ^{1}H NMR: ($CDCl_3$) 8.82 (s, 9,10-$C_{14}H_8$, 2H), 8.07 (m, $C_{14}H_8$, 2H), 7.51 (m, $C_{14}H_8$, 2H), 6.59 (s, 2,3-$C_{14}H_8$, 2H), 4.43 (t, OCH_2, J_{H-H} = 5.5, 4H), 4.02 (t, CH_2Cl, J_{H-H} = 5.5, 4H). $^{13}C\{^1H\}$ NMR: ($CDCl_3$) 148.8 (s, $C_{1/4}$), 131.8 (s, $C_{13/14}$), 128.8 (s, $C_{5/8}$), 126.0 (s, $C_{6/7}$), 125.6 (s, $C_{11/12}$), 121.1 (s, $C_{9/10}$), 102.6 (s, $C_{2/3}$), 68.8 (s, OCH_2), 42.4 (s, CH_2Cl). HRMS (EI, *m*/*z*): calcd for $C_{18}H_{16}Cl_2O_2$ 334.0527 (M^+), found 334.052 (M^+). Anal. Calcd for $C_{18}H_{16}Cl_2O_2$: C, 64.49; H, 4.81. Found: C, 63.91; H, 4.64.

General Procedure for the Synthesis of Bis[2-(diphenylphosphino)ethoxy]arenes (8−11, 13, 16). A solution of potassium diphenylphosphide (0.5 M, 8.5 mmol, 17.0 mL) in THF was added in one portion to a stirred THF solution of the appropriate chloro precursor (4.0 mmol) at RT. The reaction mixture was stirred at RT for 30 min before the solvent was removed under vacuum, resulting in a pale yellow to red, depending on precursor, residue. To this solid was added 100 mL of water followed by 100 mL of dichloromethane. The organic layer was washed with water (2 × 100 mL) and taken to dryness under vacuum. The crude product was then redissolved in a minimal amount of dichloromethane and passed through a plug of silica gel immediately before being recrystallized with pentane at −30 °C, yielding white (**8**−**11** and **13**) or pale yellow (**16**) crystals of analytically pure ligand.

1,4-Bis[2-(diphenylphosphino)ethoxy]-2-methylbenzene (8). Yield = 85%. ^{1}H NMR: (CD_2Cl_2) 7.46 (m, PC_6H_5, 8H), 7.33 (m, PC_6H_5, 12H), 6.58 (m, C_6H_3, 3H), 4.05 (m, OCH_2, 4H), 2.56 (t, CH_2P, J_{H-H} = 6.9, 2H), 2.52 (t, CH_2P, J_{H-H} = 7.8, 2H), 2.05 (s, CH_3, 3H). $^{13}C\{^1H\}$ NMR: (CD_2Cl_2) 152.9 (s, $C_{1/4}$), 151.6 (s, $C_{1/4}$), 139.1 (d, C_i-P, J_{C-P} = 9.5), 138.8 (d, C_i-P, J_{C-P} = 9.5), 133.2 (d, C_o-P, J_{C-P} = 19.1), 129.2 (s, C_p-P), 129.0 (d, C_m-P, J_{C-P} = 6.8), 128.7 (s, C_2), 118.0 (s, C_3), 112.8 (s, C_5), 112.1 (s, C_6), 66.7 (d, OCH_2, J_{C-P} = 25.3), 66.2 (d, OCH_2, J_{C-P} = 26.5), 29.0 (d, CH_2P, J_{C-P} = 12.8), 28.8 (d, CH_2P, J_{C-P} = 11.1), 16.7 (s, CH_3). $^{31}P\{^1H\}$ NMR: (CD_2Cl_2) −21.8 (s), −22.3 (s). HRMS (EI, *m*/*z*): calcd for $C_{35}H_{34}O_2P_2$ 548.2034 (M^+), found 548.2025 (M^+). Anal. Calcd for $C_{35}H_{34}P_2O_2$: C, 76.61; H, 6.25; P, 11.29. Found: C, 76.04; H, 6.20; P, 10.98.

1,4-Bis[2-(diphenylphosphino)ethoxy]-2,3-dimethylbenzene (9). Yield = 63%. ^{1}H NMR: (CD_2Cl_2) 7.48 (m, PC_6H_5, 8H), 7.34 (m, PC_6H_5, 12H), 6.51 (s, C_6H_2, 2H), 4.04 (dt (pseudo-quartet), J_{H-H} = 7.5, J_{P-H} = 9.2, OCH_2, 4H), 2.59 (t, CH_2P, J_{H-H} = 7.5, 4H), 2.06 (s, CH_3, 6H). $^{13}C\{^1H\}$ NMR: (CD_2Cl_2) 151.5 (s, $C_{1/4}$), 139.0 (d, C_i-P, J_{C-P} = 12.8), 133.2 (d, C_o-P, J_{C-P} = 19.1), 129.2 (s, C_p-P), 129.0 (d, C_m-P, J_{C-P} = 6.5), 127.5 (s, $C_{2/3}$), 109.8 (s, $C_{5/6}$), 66.9 (d, OCH_2, J_{C-P} = 24.5), 29.1 (d, CH_2P, J_{C-P} = 13.1), 12.5 (s, CH_3). $^{31}P\{^1H\}$ NMR: (CD_2Cl_2) −21.8 (s). HRMS (EI, *m*/*z*): calcd for $C_{36}H_{36}O_2P_2$ 562.2190 (M^+), found 562.2191 (M^+). Anal. Calcd for $C_{36}H_{36}P_2O_2$: C, 76.84; H, 6.45; P, 11.02. Found: C, 76.51; H, 6.43; P, 10.94.

1,4-Bis[2-(diphenylphosphino)ethoxy]-2,5-dimethylbenzene (10). Yield = 69%. ^{1}H NMR: (CD_2Cl_2) 7.46 (m, PC_6H_5, 8H), 7.35 (m, PC_6H_5, 12H), 6.50 (s, C_6H_2, 2H), 4.03 (dt (pseudo-quartet), J_{H-H} = 7.5, J_{P-H} = 7.8, OCH_2, 4H), 2.55 (t, CH_2P, J_{H-H} = 7.5, 4H), 2.02 (s, CH_3, 6H). $^{13}C\{^1H\}$ NMR: (CD_2Cl_2) 151.0 (s, $C_{1/4}$), 139.0 (d, C_i-P, J_{C-P} = 12.8), 133.2 (d, C_o-P, J_{C-P} = 19.0), 129.2 (s, C_p-P), 129.0 (d, C_m-P, J_{C-P} = 6.5), 125.1 (s, $C_{2/5}$), 115.3 (s, $C_{3/6}$), 66.9 (d, OCH_2, J_{C-P} = 25.0), 29.0 (d, CH_2P, J_{C-P} = 12.7), 16.3 (s, CH_3). $^{31}P\{^1H\}$ NMR: (CD_2Cl_2) −21.9 (s). HRMS (EI, *m*/*z*): calcd for $C_{36}H_{36}O_2P_2$ 562.2190 (M^+), found 562.2 (M^+). Anal. Calcd for $C_{36}H_{36}P_2O_2$: C, 76.84; H, 6.45; P, 11.02. Found: C, 75.90; H, 6.41; P, 11.02.

1,4-Bis[2-(diphenylphosphino)ethoxy]-2,3,5-trimethylbenzene (11). Yield = 69%. ^{1}H NMR: (CD_2Cl_2) 7.48 (m, PC_6H_5, 8H), 7.36 (m, PC_6H_5, 12H), 6.41 (s, C_6H, 1H), 4.06 (dt (pseudo-quartet), J_{H-H} = 7.8, J_{P-H} = 7.8, OCH_2, 2H), 3.78 (dt (pseudo-quartet), J_{H-H} = 7.8, J_{P-H} = 7.5, OCH_2, 2H), 2.63 (t, CH_2P, J_{H-H} = 7.8, 2H), 2.59 (t, CH_2P, J_{H-H} = 7.2, 2H), 2.14 (s, CH_3, 3H), 2.11 (s, CH_3, 3H), 2.01 (s, CH_3, 3H). $^{13}C\{^1H\}$ NMR: (CD_2Cl_2) 153.0 (s, $C_{1/4}$), 150.3 (s, $C_{1/4}$), 139.0 (d, C_i-P, J_{C-P} = 13.1), 138.9 (d, C_i-P, J_{C-P} = 13.1), 133.2 (d, C_o-P, J_{C-P} = 19.0), 133.1 (d, C_o-P, J_{C-P} = 19.3), 131.2 (s, C_3), 129.6 (s, C_p-P), 129.5 (d, C_m-P, J_{C-P} = 6.6), 128.5 (s, C_5), 124.5 (s, C_2), 112.4 (s, C_6), 70.4 (d, OCH_2, J_{C-P} = 24.1), 66.7 (d, OCH_2, J_{C-P} = 23.9), 30.3 (d, CH_2P, J_{C-P} = 13.6), 29.7 (d, CH_2P, J_{C-P} = 13.9), 16.8 (s, CH_3), 13.3 (s, CH_3), 12.3 (s, CH_3). $^{31}P\{^1H\}$ NMR: (CD_2Cl_2) −20.6 (s), −21.2 (s). HRMS (EI, *m*/*z*): calcd for $C_{37}H_{38}O_2P_2$ 576.2347 (M^+), found 576.2356 (M^+).

1,4-Bis[2-(diphenylphosphino)ethoxy]-2,5-di-*tert*-butylbenzene (13). Yield = 67%. ^{1}H NMR: (CD_2Cl_2) 7.46 (m, PC_6H_5, 8H), 7.34 (m, PC_6H_5, 12H), 6.69 (s, C_6H_2, 2H), 4.06 (dt (pseudo-quartet), J_{H-H} = 7.6, J_{P-H} = 7.8, OCH_2, 4H), 2.60 (t, CH_2P, J_{H-H} = 7.6, 4H), 1.30 (s, $C(CH_3)_3$, 18H). $^{13}C\{^1H\}$ NMR: (CD_2Cl_2) 151.5 (s, $C_{1/4}$), 138.8 (d, C_i-P, J_{C-P} = 12.8), 136.8 (s, $C_{2/5}$), 133.2 (d, C_o-P, J_{C-P} = 19.1), 129.3 (s, C_p-P), 129.1 (d, C_m-P, J_{C-P} = 6.8), 112.8 (s, $C_{3/6}$), 66.6 (d, OCH_2, J_{C-P} = 26.5), 35.0 (s, $C(CH_3)_3$), 30.2 (s, $C(CH_3)_3$), 29.3 (d, CH_2P, J_{C-P} = 13.4). $^{31}P\{^1H\}$ NMR: (CD_2Cl_2) −22.9 (s). HRMS (EI, *m*/*z*): calcd for $C_{42}H_{48}O_2P_2$ 646.3129 (M^+), found 646.3139 (M^+). Anal. Calcd for $C_{42}H_{48}O_2P_2$: C, 77.98; H, 7.48; P, 9.58. Found: C, 78.00; H, 7.51; P, 9.58.

1,4-Bis[2-(diphenylphosphino)ethoxy]anthracene (16). Yield = 66%. ^{1}H NMR: (CD_2Cl_2) 8.51 (s, 9,10-$C_{14}H_8$, 2H), 7.93 (m, 5,8-$C_{14}H_8$, 2H), 7.55 (m, PC_6H_5, 8H), 7.47 (m, 6,7-$C_{14}H_8$, 2H), 7.38 (m, PC_6H_5, 12H), 6.46 (s, 2,3-$C_{14}H_8$, 2H), 4.32 (m, OCH_2, 4H), 2.77 (t, CH_2P, J_{H-H} = 6.7, 4H). $^{13}C\{^1H\}$ NMR: (CD_2Cl_2) 149.0 (s, $C_{1/4}$), 139.1 (d, C_i-P, J_{C-P} = 13.1), 133.3 (d, C_o-P, J_{C-P} = 18.8), 131.8 (s, $C_{13/14}$), 129.3 (s, C_p-P), 129.1 (d, C_m-P, J_{C-P} = 6.8), 129.0 (s, $C_{5/8}$), 126.0 (s, $C_{6/7}$), 125.9 (s, $C_{9/10}$), 121.2 (s, $C_{11/12}$), 102.5 (s, $C_{2/3}$), 66.6 (d, OCH_2, J_{C-P} = 23.9), 28.9 (d, CH_2P, J_{C-P} = 13.7). $^{31}P\{^1H\}$ NMR: (CD_2Cl_2) −21.0 (s). HRMS (EI, *m*/*z*): calcd for $C_{42}H_{36}O_2P_2$ 634.2190 (M^+), found 634.2173 (M^+). Anal. Calcd for $C_{42}H_{36}O_2P_2$: C, 79.47; H, 5.72; P, 9.77. Found: C, 79.37; H, 5.61; P, 10.09.

General Procedure for the Synthesis of Condensed Intermediates (18−21, 23, 26). In a glovebox $[Rh(Cl)(COE)_2]_2$ (40 mg, 1.13 × 10^{-4} mol) and $AgBF_4$ (22 mg, 1.13 × 10^{-4} mol) were reacted in 3 mL of CH_2Cl_2 for 30 min. The resulting reaction mixture was filtered through Celite, and the filtrate was diluted with 125 mL of THF. A solution of the appropriate ligand (1.129 × 10^{-4} mol) in 125 mL of THF was added dropwise to this solution at −78 °C over 1 h and then warmed to room temperature over 1 h. The solvent was removed under vacuum to yield an orange-red powder. The solid was dissolved in a small amount of CH_2Cl_2 and precipitated with pentane. The resulting orange-red solid was collected over Celite and redissolved in CH_2Cl_2. A few drops of CH_3CN were added to this solution and stirred for 20 min at room temperature. The solvent was pumped off in vacuo, and the resulting solid was dried overnight at 55 °C under vacuum.

[μ^2,η^1:η^6:η^1-(1,4-Bis(2-(diphenylphosphino)ethoxy)-2-methylbenzene)$_2$Rh$_2$][BF_4]$_2$ (18b). Yield = 92%. ^{1}H NMR: (CD_2Cl_2) 8.36 (m, C_6H_3, 4H), 8.11 (m, PC_6H_5, 4H), 7.80 (m, PC_6H_5, 8H), 7.58 (m, PC_6H_5, 10H), 7.12 (m, PC_6H_5, 2H), 7.00 (m, PC_6H_5, 2H), 6.91 (m, PC_6H_5, 6H), 6.75 (m, PC_6H_5, 4H), 6.51 (m, C_6H_3, 2H), 6.32 (m, PC_6H_5, 8H), 4.91 (m, OCH_2, 2H), 4.26 (m, OCH_2, 2H), 3.82 (m, OCH_2, 2H), 3.60 (m, OCH_2, 2H), 2.67 (m, CH_3, 3H), 2.38 (m, CH_2P, 4H), 1.88 (m, CH_2P, 4H), 1.61 (m, CH_3, 3H). $^{31}P\{^1H\}$ NMR (CD_2Cl_2): 28.7 (dd (pseudo-ddd), J_{P-P} = 39, J_{Rh-P} = 213), 28.9 (dd (pseudo-ddd), J_{P-P} = 39, J_{Rh-P} = 213), 34.0 (dd (pseudo-ddd), J_{P-P} = 39, J_{Rh-P} = 206), 34.8 (dd (pseudo-ddd), J_{P-P} = 39, J_{Rh-P} = 206). MS (ESI, *m*/*z*): $[M - BF_4^-]^+$ = 1389.3 (calcd for $C_{70}H_{68}BF_4O_4P_4Rh_2^+$ = 1389.2), $[M - 2BF_4^-]^{2+}$ = 651.3 (calcd for $C_{70}H_{68}O_4P_4Rh_2^{2+}$ = 651.1). Anal. Calcd for $C_{70}H_{68}B_2F_8O_4P_4Rh_2$: C, 56.90; H, 4.64; P, 8.39. Found: C, 55.98; H, 4.65; P, 8.29.

[μ^2,η^1:η^6:η^1-(1,4-Bis(2-(diphenylphosphino)ethoxy)-2,3-dimethylbenzene)$_2$Rh$_2$][BF_4]$_2$ (19b). Yield = 95%. ^{1}H NMR: (CD_2Cl_2) 8.30 (d, C_6H_2, J_{H-H} = 9.6, 2H), 8.12 (m, PC_6H_5, 4H), 7.76 (m, PC_6H_5, 8H), 7.63 (m, PC_6H_5, 2H), 7.45 (m, PC_6H_5, 8H), 7.08 (m, PC_6H_5, 2H), 6.96 (m, PC_6H_5, 2H), 6.84 (m, PC_6H_5, 6H), 6.72 (m, PC_6H_5, 4H), 6.50 (d, C_6H_2, J_{H-H} = 9.5, 2H), 6.36 (m, PC_6H_5, 4H), 5.00 (m, OCH_2, 2H), 4.39 (m, OCH_2, 2H), 3.82 (m, OCH_2, 2H), 3.62 (m, OCH_2, 2H), 2.68 (m, CH_2P, 2H), 2.61 (s, CH_3, 6H), 2.41 (m, CH_2P, 2H), 2.18 (m, CH_2P, 2H), 1.82 (m, CH_2P, 2H), 1.60 (s, CH_3, 6H). $^{31}P\{^1H\}$ NMR (CD_2Cl_2): 29.7 (dd, J_{P-P} = 41, J_{Rh-P} = 213), 33.9 (dd, J_{P-P} = 40, J_{Rh-P} = 206). MS (ESI, *m*/*z*): $[M - BF_4^-]^+$ = 1417.4 (calcd for $C_{72}H_{72}BF_4O_4P_4Rh_2^+$ = 1417.3), $[M - 2BF_4^-]^{2+}$ = 665.2 (calcd for $C_{72}H_{72}O_4P_4Rh_2^{2+}$ = 665.1). Anal. Calcd for $C_{72}H_{72}B_2F_8O_4P_4Rh_2$: C, 57.44; H, 4.82; P, 8.24. Found: C, 57.42; H, 4.86; P, 8.71.

[μ^2,η^1:η^6:η^1-(1,4-Bis(2-(diphenylphosphino)ethoxy)-2,5-dimethylbenzene)$_2$Rh$_2$][BF$_4$]$_2$ (20b). Yield = 90%. ^{1}H NMR: (CD_2Cl_2) 8.05 (s, C_6H_2, 2H), 7.78 (m, PC_6H_5, 4H), 7.67 (m, PC_6H_5, 4H), 7.54 (m, PC_6H_5, 6H), 7.38 (m, PC_6H_5, 6H), 7.08 (m, PC_6H_5, 12H), 6.82 (m, PC_6H_5, 4H), 6.49 (m, PC_6H_5, 4H), 5.33 (s, C_6H_2, 2H), 4.82 (m, OCH_2, 2H), 4.38 (m, OCH_2, 4H), 3.66 (m, OCH_2, 2H), 2.37 (s, CH_3, 6H), 2.32 (m, CH_2P, 2H), 2.10 (m, CH_2P, 2H), 1.84 (m, CH_2P, 2H), 1.77 (s, CH_3, 6H), 1.58 (m, CH_2P, 2H). $^{31}P\{^1H\}$ NMR (CD_2Cl_2): 26.2 (dd, J_{P-P} = 40, J_{Rh-P} = 213), 36.2 (dd, J_{P-P} = 40, J_{Rh-P} = 207). MS (ESI, *m*/*z*): $[M - BF_4^-]^+$ = 1417.4 (calcd for $C_{72}H_{72}BF_4O_4P_4Rh_2^+$ = 1417.3), $[M - 2BF_4^-]^{2+}$ = 665.6 (calcd for $C_{72}H_{72}O_4P_4Rh_2^{2+}$ = 665.1).

[κ^2:μ^2:κ^2-(1,4-Bis(2-(diphenylphosphino)ethoxy)-2,3,5-trimethylbenzene)$_2$Rh$_2$][BF$_4$]$_2$ (21a). Yield = 91%. ^{1}H NMR: (CD_2Cl_2) 7.71 (m, PC_6H_5, 16H), 7.51 (m, PC_6H_5, 8H), 7.42 (m, PC_6H_5, 16H), 6.79 (s, C_6H, 2H), 3.95 (m, OCH_2, 4H), 3.67 (m, OCH_2, 4H), 2.66 (m, CH_2P, 8H), 2.41 (s, CH_3, 6H), 2.37 (s, CH_3, 6H), 2.23 (s, CH_3, 6H). $^{31}P\{^1H\}$ NMR (CD_2Cl_2): 61.5 (dd, J_{P-P} = 40, J_{Rh-P} = 215), 62.1 (dd, J_{P-P} = 40, J_{Rh-P} = 215). MS (ESI, *m*/*z*): $[M - BF_4^-]^+$ = 1445.1 (calcd for $C_{74}H_{76}BF_4O_4P_4Rh_2^+$ = 1445.3), $[M - 2BF_4^-]^{2+}$ = 679.5 (calcd for $C_{74}H_{76}O_4P_4Rh_2^{2+}$ = 679.1).

[μ^2,η^1:η^6:η^1-(1,4-Bis(2-(diphenylphosphino)ethoxy)-2,5-di-*tert*-butylbenzene)$_2$Rh$_2$][BF$_4$]$_2$ (23b). Yield = 88%. ^{1}H NMR: (CD_2Cl_2) 8.12−7.08 (m, PC_6H_5, 32H), 6.83 (m, PC_6H_5, 4H), 6.51 (m, PC_6H_5, 4H), 6.20 (m, C_6H_2, 2H), 5.58 (m, C_6H_2, 2H), 4.61 (m, OCH_2, 2H), 4.03 (m, OCH_2, 2H), 3.76 (m, OCH_2, 2H), 3.39 (m, OCH_2, 2H), 2.83 (m, CH_2P, 2H), 2.62 (m, CH_2P, 2H), 2.10 (m, CH_2P, 2H), 1.66 (m, $CH_2P + C(CH_3)_3$, 20H), 1.35 (m, $C(CH_3)_3$, 18H). $^{31}P\{^1H\}$ NMR (CD_2Cl_2): 19.4 (dd, J_{P-P} = 40, J_{Rh-P} = 214), 23.1 (dd, J_{P-P} = 40, J_{Rh-P} = 198). MS (ESI, *m*/*z*): $[M - 2BF_4^-]^{2+}$ = 749.8 (calcd for $C_{84}H_{96}O_4P_4Rh_2^{2+}$ = 749.2).

[μ^2,η^1:η^6:η^1-(1,4-Bis(2-(diphenylphosphino)ethoxy)-1,4-anthracene)$_2$Rh$_2$][BF$_4$]$_2$ (26b). Yield = 93%. ^{1}H NMR: (CD_2Cl_2) 8.92 (s, $C_{14}H_8$, 2H), 8.62 (m, $C_{14}H_8$, 2H), 8.43 (m, $C_{14}H_8$, 2H), 8.31−6.41 (m, PC_6H_5, 40H), 8.03 (m, $C_{14}H_8$, 2H), 6.35 (m, $C_{14}H_8$, 2H), 6.30 (m, $C_{14}H_8$, 2H), 6.08 (m, $C_{14}H_8$, 2H), 5.93 (m, $C_{14}H_8$, 2H), 5.39 (m, OCH_2, 2H), 5.01 (m, OCH_2, 2H), 4.06 (m, OCH_2, 2H), 3.66 (m, OCH_2, 2H), 2.82 (m, CH_2P, 2H), 2.51 (m, CH_2P, 2H), 2.09 (m, CH_2P, 4H). $^{31}P\{^1H\}$ NMR (CD_2Cl_2): 20.5 (dd, J_{P-P} = 37, J_{Rh-P} = 206), 30.7 (dd, J_{P-P} = 37, J_{Rh-P} = 206). MS (ESI, *m*/*z*): $[M - BF_4^-]^+$ = 1562.2 (calcd for $C_{84}H_{72}BF_4O_4P_4Rh_2^+$ = 1562.0).

X-ray Crystallography. Diffraction intensity data were collected with Bruker SMART-1000 (**18b**) and SMART APEX (**19b** and **23b**) CCD diffractometers equipped with a graphite-monochromated Mo Kα radiation source. The data collected were processed to produce conventional intensity data by the program SAINT-NT (Bruker). The intensity data were corrected for Lorentz and polarization effects. Absorption correction was applied using the SADABS[16] empirical method (T_{min}/T_{max} = 0.82 (**18b**), 0.83 (**19b**), and 0.69 (**23b**)). The structures were solved by direct methods provided by the program package SIR92[17] (**18b**) and using the Patterson function (**19b** and **23b**) completed by subsequent difference Fourier syntheses and refined by full matrix least-squares procedures on F^2. Unless otherwise noted, all the non-hydrogen atoms were refined anisotropically. Hydrogen atom positions were calculated and included in the final cycle of refinement. The Flack parameter for **19b** is 0.19(3). Crystal data, data collection, and refinement parameters are given in Table 2.

The maximum and minimum peaks on the final difference Fourier map in **18b** correspond to 2.72 and −0.86 e$^-$/Å^3 and were located in the vicinity of the disordered solvent molecules, respectively. In **19b** and **23b**, the highly disordered CH_2Cl_2 and diethyl ether solvate molecules were treated by SQUEEZE.[18] Corrections of the X-ray data by SQUEEZE (904 and 1237 e$^-$/cell, respectively for **19b** and **23b**) were close to the required values (840 and 1184 e$^-$/cell for two CH_2Cl_2 and five diethyl ether molecules in **19b**; six CH_2Cl_2 and one diethyl ether molecule in **23b**).

For **18b**, all calculations were performed using the teXsan crystallographic software package of Molecular Structure Corporation except for refinement, which was performed using SHELXL-97.[19] For **19b** and **23b** all calculations were performed by the SHELXTL (5.10) program package.

Acknowledgment. C.A.M. acknowledges the NSF (CHE-0071885/001) and AFOSR (F49620-00-1-0230) for support of this research. B.J.H. acknowledges Sigma Xi, the Link Foundation, and NSF/NSEC (EEC-0118025) for fellowship support. P.A.U. acknowledges the ETH Zurich-Northwestern University exchange program for the research opportunity. A.L.R. acknowledges the NSF for their support of the purchase of the CCD-based diffractometer (CHE00091968).

Supporting Information Available: Crystallographic data for **18b**, **19b**, and **23b** in tabular (pdf) and cif file format are available free of charge via the Internet at http://pubs.acs.org.

OM030611A

(16) Sheldrick, G. M. *SADABS* (2.01), Bruker/Siemens Area Detector Absorption Correction Program; Bruker AXS: Madison, WI, 1998.
(17) Altomare, A.; Cascarano, G.; Giacovazzo, C.; Guagliardi, A. *J. Appl. Crystallogr.* **1994**, *27*, 1045−1050.
(18) Van der Sluis, P.; Spek, A. L. *Acta Crystallogr.* **1990**, *A46*, 194−201.
(19) Sheldrick, G. M. *SHELXL-97*, Program for Crystal Structure Solution; Institüt für Anorganische Chemie der Universität, Tammanstrasse 4, D-3400 Gottingen, Germany, 1997.